

DESY 07-183
SFB/CPP-07-70

FERMIONIC NNLO CONTRIBUTIONS TO BHABHA SCATTERING *

S. ACTIS^a, M. CZAKON^{bc}, J. GLUZA^c, T. RIEMANN^a

^a Deutsches Elektronen-Synchrotron DESY
Platanenallee 6, D-15738 Zeuthen, Germany

^b Institut für Theoretische Physik und Astrophysik, Universität Würzburg
Am Hubland, D-97074 Würzburg, Germany

^c Institute of Physics, Univ. of Silesia, Uniwersytecka 4, 40007 Katowice, Poland

We derive the two-loop corrections to Bhabha scattering from heavy fermions using dispersion relations. The double-box contributions are expressed by three kernel functions. Convoluting the perturbative kernels with fermionic threshold functions or with hadronic data allows to determine numerical results for small electron mass m_e , combined with arbitrary values of the fermion mass m_f in the loop, $m_e^2 \ll s, t, m_f^2$, or with hadronic insertions. We present numerical results for $m_f = m_\mu, m_\tau, m_{top}$ at typical small- and large-angle kinematics ranging from 1 GeV to 500 GeV.

1. Introduction

Bhabha scattering is one of the theoretically best studied scattering processes at e^+e^- colliders and can also be measured with a high precision.

* Presented by T.R. at XXXI Conference of Theoretical Physics “Matter to the Deepest: Recent Developments In Physics of Fundamental Interactions”, Ustroń, Poland, 5-11 September 2007 [1]. Work supported in part by Sonderforschungsbereich/Transregio TRR 9 of DFG “Computergestützte Theoretische Teilchenphysik”, by the Sofja Kovalevskaja Award of the Alexander von Humboldt Foundation sponsored by the German Federal Ministry of Education and Research, and by the European Community’s Marie-Curie Research Training Networks MRTN-CT-2006-035505 “HEPTOOLS” and MRTN-CT-2006-035482 “FLAVIANet”.

The accuracy of the Monte-Carlo programs developed originally for physics at LEP is about 10^{-3} , and with a complete two-loop calculation one may reach 10^{-4} . The latter number is indicative of efforts for the International Linear Collider (ILC), here especially in the GigaZ option running at the Z boson resonance, but also for meson factories running at much smaller energies of about 1 or 10 GeV.

Recent years brought considerable progress in the determination of the virtual NNLO corrections. The virtual $O(\alpha^2)$ contributions to the massless differential Bhabha cross section have been determined in [2]. Shortly after, this result was used for deriving the $O(\alpha^2 L)$ ($L = \ln(s/m_e^2)$) corrections to massive Bhabha scattering in [3]. The missing photonic correction terms of order $O(\alpha^2 L^0)$ were derived, also from [2], in [4, 5]. The virtual corrections from fermion loop insertions, including the corresponding double-box diagrams, could not be covered by that method. For $n_f = 1$, *i.e.* the case of only electron loops, the corresponding diagrams were evaluated analytically in [6, 7, 8, 9], and the net $n_f = 1$ cross section in [10, 11].

At this stage the numerically most important two-loop corrections were known. For a complete treatment one needs additionally the $n_f = 2$ two-loop corrections with heavy fermion insertions, including the hadronic corrections which replace the loop insertions from light quarks. The leptonic $n_f = 2$ contributions have been derived quite recently in two papers in the limit $m_e^2 \ll m_f^2 \ll s, t$; with a direct Feynman diagram calculation in [12], and using a factorization formula that relates massless and massive amplitudes in [13] (for that method see also [14]).

It might be interesting to mention that the original expectations on the necessity of a complete, direct two-loop massive Feynman diagram evaluation were not fulfilled. After the analytical evaluation of a massive planar and a massive non-planar double-box diagram (both with seven propagators) in [15] and in [16], resp., there was hope to evaluate all the remaining diagrams soon. There are 33 two-loop box master integrals, nine of them with seven lines [17]. In fact, from recent studies on the exact and mass expanded treatment of two-loop box master integrals in [18] and [19], resp., it became clear that an evaluation of all the massive master integrals is a more complicated task than was expected. Quite recently, the case of non-planar master integrals was successfully treated in another, but related context [20]. Proceeding similarly for Bhabha scattering seems feasible now. As a matter of fact, due to these reasons, the direct Feynman diagram approach was not used for the phenomenologically needed two-loop predictions and the above-mentioned papers [15]- [19] remained so far a mere interesting, challenging theoretical development.

In this paper, we report on the evaluation of the leptonic $n_f = 2$ two-loop contributions with *arbitrary mass* of the heavier fermion, *i.e.* exploring

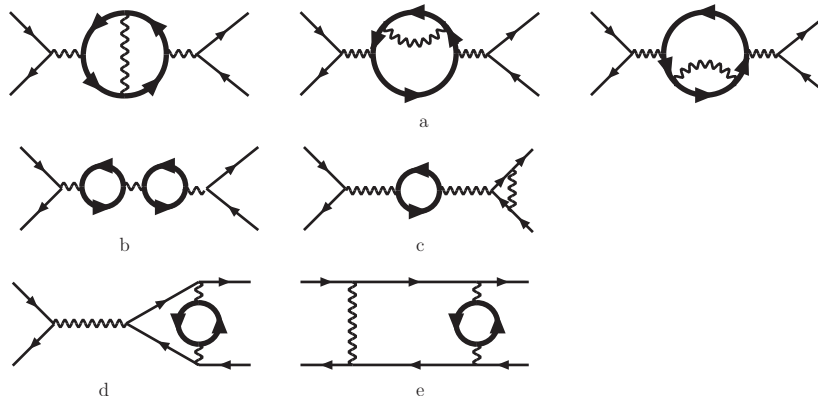


Fig. 1. Classes of two-loop diagrams for Bhabha scattering containing at least one fermion loop.

the extended kinematical region $m_e^2 \ll m_f^2, s, t$. We use the dispersion approach, so that our formulae may be applied without further modification also to hadronic corrections.

For a review on the status of Monte-Carlo studies for Bhabha scattering at this conference we refer to [21], and for a discussion on progress related to radiative loop corrections to [22].

2. Formulae

The classes of two-loop $n_f = 2$ corrections are shown in Figure 1. The four direct and four crossed fermionic two-loop box diagrams, obtained applying proper permutations to the sample diagram shown in Figure 1, are infrared (IR) divergent, and they have to be combined with other IR-divergent factorizable corrections in order to get an IR-finite contribution to the cross section. In particular, we have to add the interference of two-loop box (class e) and reducible vertex diagrams (class c) with the tree-level amplitude to the interference of one-loop vertex and box diagrams with one-loop vacuum polarization diagrams. Finally, we construct an IR-finite quantity taking into account also the real emission of one soft photon from one-loop vacuum polarization diagrams. Sample contributions are given in Figure 2.

The net contribution of pure self-energy corrections (classes a – b), irreducible vertex diagrams (class d), and the aforementioned IR-divergent contributions reads as

$$\frac{d\sigma^{\text{NNLO,ferm.}}}{d\Omega} = \frac{d\sigma^{\text{a,b}}}{d\Omega} + \frac{d\sigma^{\text{d}}}{d\Omega} + \frac{d\sigma^{\text{rest}}}{d\Omega}, \quad (1)$$

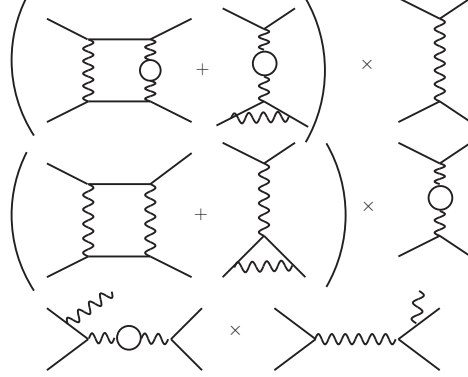


Fig. 2. The fermionic two-loop boxes combine with other diagrams to an infrared-finite cross-section contribution.

where $d\sigma^{\text{rest}}/d\Omega$ can be splitted in two components,

$$\frac{d\sigma^{\text{rest}}}{d\Omega} = \frac{d\sigma^{\text{box}}}{d\Omega} + \frac{d\sigma^{\text{fact.}}}{d\Omega}. \quad (2)$$

We concentrate now on the renormalized two-loop box diagrams of class e, whose total contribution to the cross section may be written as

$$\frac{d\sigma^{\text{box}}}{d\Omega} = \left(\frac{\alpha}{\pi}\right)^2 \frac{\alpha^2}{2s} \left(\frac{m_e^2}{s} \text{Re } A_s + \frac{m_e^2}{t} \text{Re } A_t \right). \quad (3)$$

Here the auxiliary functions A_s and A_t can be conveniently expressed through three independent form factors B_i , with $i = A, B, C$, evaluated with different kinematical arguments,

$$\begin{aligned} A_s &= B_A(s, t) + B_B(t, s) + B_C(u, t) - B_B(u, s), \\ A_t &= B_B(s, t) + B_A(t, s) - B_B(u, t) + B_C(u, s). \end{aligned} \quad (4)$$

The particular contribution of the diagram of Figure 1 coming from the interference with the tree-level s-channel is $B_A(s, t)$, and from the t-channel is $B_B(s, t)$.

For the evaluation of hadronic corrections, we observe that each term of Eq. (4) can be written through the convolution of a kernel function K_I , $I = A, B, C$, with the hadronic cross-section ratio R_{had} ,

$$B_{I, had}(s, t) = \int_{4M_\pi^2}^{\infty} \frac{dz}{z} R_{had}(z) K_I(s, t, z). \quad (5)$$

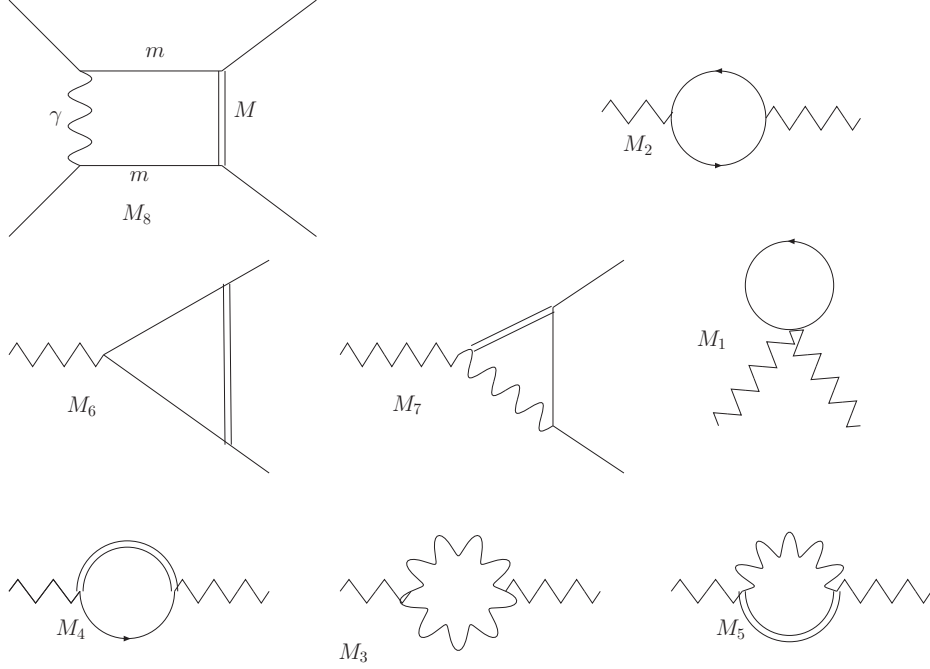


Fig. 3. The master integrals for the two-loop box kernel functions.

For leptons and the top quark, we have to replace $4 M_\pi^2 \rightarrow 4 m_f^2$ and $R_{had} \rightarrow R_{fer}$, given by

$$R_{fer}(z) = Q_f^2 C_f \sqrt{1 - 4 \frac{m_f^2}{z}} \left(1 + 2 \frac{m_f^2}{z} \right) + \epsilon R_{fer}^\epsilon(z), \quad (6)$$

where Q_f is the electric charge in units of $|e|$ and C_f is the color factor. Being the box diagrams IR divergent, and showing poles in ϵ , one should take into account higher orders in ϵ for R . However, after assembling box diagrams with factorizable corrections, IR poles cancel and R can be evaluated at order ϵ^0 .

The three box kernels are our main technical result. They have been derived with the aid of the master integrals of Figure 3, in the limit $m_e^2 \ll m_f^2, s, t$. The master integrals were determined with `IdSolver` and evaluated with the Mathematica packages `ambre` [23] and `MB` [24], and eventually mass expanded with a Mathematica package. We also made use of `FORM` [25]. We

reproduce one of the kernels here,¹

$$\begin{aligned}
K_C(x, y, z) = & \frac{1}{3 m_e^2 (y - z)} \left\{ 2 \frac{F_\epsilon}{\epsilon} x^2 L_x + 4 \zeta_2 x^2 \left(\frac{z}{y} - 2 \right) - 2 (x^2 + y^2 \right. \\
& + x y) L_x + x^2 \left(\frac{z}{y} - 1 \right) L_y + 2 x^2 \left(\frac{z}{y} - 1 \right) L_y^2 + 4 x^2 L_x L_y \\
& + x^2 \left(\frac{z}{y} - 1 \right) \ln \left(\frac{z}{m_e^2} \right) - 2 x^2 \left(\frac{z}{y} - \frac{1}{2} \right) \ln^2 \left(\frac{z}{m_e^2} \right) + 4 x^2 \left(\frac{z}{y} \right. \\
& - 1 \left. \right) \ln \left(\frac{z}{m_e^2} \right) \ln \left(1 - \frac{z}{y} \right) + 2 x^2 \ln \left(\frac{z}{m_e^2} \right) L_x - x^2 \left(\frac{z}{y} + \frac{y}{z} \right. \\
& - 2 \left. \right) \ln \left(1 - \frac{z}{y} \right) - 4 x^2 \ln \left(1 - \frac{z}{y} \right) L_x + 4 x^2 \left(\frac{z}{y} - 1 \right) \text{Li}_2 \left(\frac{z}{y} \right) \\
& \left. - 2 x^2 \text{Li}_2 \left(1 + \frac{z}{x} \right) \right\}, \tag{7}
\end{aligned}$$

where $L_x = \ln(-m_e^2/x)$, $L_y = \ln(-m_e^2/y)$ and F_ϵ is the normalization factor

$$F_\epsilon = \left(\frac{m_e^2 \pi e^{\gamma_E}}{\mu^2} \right)^{-\epsilon}. \tag{8}$$

Here μ is the 't Hooft mass unit and γ_E is the Euler-Mascheroni constant.

3. Numerical Results

The sum of the box contributions with IR-divergent factorizable corrections (see Figure 2 for sample cases) is infrared-finite and can be cast in the following form,

$$\begin{aligned}
\frac{d\sigma^{\text{rest}}}{d\Omega} = & \left(\frac{\alpha}{\pi} \right)^2 \frac{\alpha^2}{s} \left\{ \int_{4M^2}^{\infty} dz \frac{R(z)}{z} \frac{1}{t - z} F_1(z) \right. \\
& + \text{Re} \int_{4M^2}^{\infty} dz \frac{R(z)}{z} \frac{1}{s - z + i\delta} \left[F_2(z) + F_3(z) \ln \left(1 - \frac{z}{s + i\delta} \right) \right] \\
& \left. + \pi \text{Im} \int_{4M^2}^{\infty} dz \frac{R(z)}{z} \frac{1}{s - z + i\delta} F_4(z) \right\}. \tag{9}
\end{aligned}$$

We may show here one of the auxiliary functions $F_i(z)$,

$$\begin{aligned}
F_1(z) = & \frac{1}{3} \left\{ \left[3 \left(\frac{t^2}{s} + 2 \frac{s^2}{t} \right) + 9 (s + t) \right] \ln \left(\frac{s}{m_e^2} \right) + \left[-z^2 \left(\frac{1}{s} + \frac{2}{t} + 2 \frac{s}{t^2} \right) \right. \right. \\
& \left. \left. + z \left(4 + 4 \frac{s}{t} + 2 \frac{t}{s} \right) + \frac{1}{2} \frac{t^2}{s} + 6 \frac{s^2}{t} + 5s + 4t \right] \ln \left(-\frac{t}{s} \right) + s \left(-\frac{z}{t} + \frac{3}{2} \right) \right\}
\end{aligned}$$

¹ Some formulae have to be omitted here due to limited space; they may be found at the webpage <http://www-zeuthen.desy.de/theory/research/bhabha/bhabha.html>.

$$\begin{aligned}
& \times \ln\left(1 + \frac{t}{s}\right) + \left[\frac{1}{2} \frac{z^2}{s} + 2z\left(1 + \frac{s}{t}\right) - \frac{11}{4}s - 2t\right] \ln^2\left(-\frac{t}{s}\right) \\
& - \left[\frac{1}{2} \frac{z^2}{t} - z\left(1 + \frac{s}{t}\right) + \frac{t^2}{s} + 2\frac{s^2}{t} + \frac{9}{2}s + \frac{15}{4}t\right] \ln^2\left(1 + \frac{t}{s}\right) \\
& + \left[\frac{z^2}{t} - 2z\left(1 + \frac{s}{t}\right) + 2\frac{s^2}{t} + 5s + \frac{5}{2}t\right] \ln\left(-\frac{t}{s}\right) \ln\left(1 + \frac{t}{s}\right) \\
& - 4\left[\frac{t^2}{s} + 2\frac{s^2}{t} + 3(s+t)\right] \left[1 + \text{Li}_2\left(-\frac{t}{s}\right)\right] \\
& - \left[2\frac{z^2}{t} - 4z\left(1 + \frac{s}{t}\right) - 4\frac{t^2}{s} - 2\frac{s^2}{t} + s - \frac{11}{2}t\right] \zeta_2 \\
& - \left[\frac{t^2}{s} + 2\frac{s^2}{t} + 3(s+t)\right] \ln\left(\frac{z}{s}\right) \ln\left(1 + \frac{t}{s}\right) + \left[z^2\left(\frac{1}{s} + 2\frac{s}{t^2} + \frac{2}{t}\right) \right. \\
& \left. - z\left(\frac{t}{s} + 2\frac{s}{t} + 2\right)\right] \ln\left(\frac{z}{s}\right) - \left[z^2\left(\frac{1}{s} + \frac{1}{t}\right) + 2z\left(1 + \frac{s}{t}\right) + s + 2\frac{s^2}{t}\right] \\
& \times \ln\left(\frac{z}{s}\right) \ln\left(1 + \frac{z}{s}\right) + \left[\frac{z^2}{s} + 4z\left(1 + \frac{s}{t}\right) - \frac{t^2}{s} - 4(s+t)\right] \\
& \times \ln\left(\frac{z}{s}\right) \ln\left(1 - \frac{z}{t}\right) - \left[z^2\left(\frac{1}{s} + 2\frac{s}{t^2} + \frac{2}{t}\right) - 2z\left(\frac{t}{s} + 2\frac{s}{t} + 2\right) + \frac{t^2}{s} \right. \\
& \left. + 2(s+t)\right] \ln\left(1 - \frac{z}{t}\right) + \left[\frac{z^2}{t} - 2z\left(1 + \frac{s}{t}\right) + 2\frac{t^2}{s} + 8s + 4\frac{s^2}{t} + 7t\right] \\
& \times \ln\left(1 - \frac{z}{t}\right) \ln\left(1 + \frac{t}{s}\right) - \left[z^2\left(\frac{1}{s} + \frac{1}{t}\right) + 2z\left(1 + \frac{s}{t}\right) + s + 2\frac{s^2}{t}\right] \\
& \times \text{Li}_2\left(-\frac{z}{s}\right) + \left[\frac{z^2}{s} + 4z\left(1 + \frac{s}{t}\right) - \frac{t^2}{s} - 4(s+t)\right] \text{Li}_2\left(\frac{z}{t}\right) \\
& - \left[\frac{z^2}{t} - 2z\left(1 + \frac{s}{t}\right) + \frac{t^2}{s} + 5s + 2\frac{s^2}{t} + 4t\right] \text{Li}_2\left(1 + \frac{z}{u}\right)\} \\
& + 4\left(\frac{1}{3}\frac{t^2}{s} + \frac{2}{3}\frac{s^2}{t} + s + t\right) \ln\left(\frac{2\omega}{\sqrt{s}}\right) \left[\ln\left(\frac{s}{m_e^2}\right) + \ln\left(-\frac{t}{s}\right) \right. \\
& \left. - \ln\left(1 + \frac{t}{s}\right) - 1\right]. \tag{10}
\end{aligned}$$

Table 1 and Table 2 contain numerical results for small- and large-angle scattering at a variety of energy scales. We report the QED tree-level prediction, as well as the process-dependent contributions at NNLO of Eq. (9); in other words, we exclude from the tables pure self-energy corrections, which can be described introducing a running fine-structure constant and were deeply investigated in the past (see [26]), and irreducible vertex contributions (see [27] and [28]). A complete phenomenological analysis requires also to add the corresponding terms arising from unresolved real fermion pair production.

The Standard Model cross sections shown here rely on Born formulae with Z boson and photon exchange a la **Zfitter** [29, 30]. Moreover, although the contributions from electron loops have been obtained by exact (in m_e) evaluation of the Feynman diagrams, we report here for consistency the approximated results for $m_e \ll s, t$.

We further compare the analytical results of [12] with those obtained with the dispersion approach and it is nicely seen that the former approach the latter in regions where the former are expected to become good approximations. In both tables, for each fermion flavour, we show the result obtained through the dispersion-based approach (first line) and the one coming from the analytical expansion (second line), neglecting $\mathcal{O}(m_f^2/x)$, where $x = s, |t|, |u|$. When $m_f^2 > x$, the entry is suppressed. We switch off in the tables the effect of the logarithm containing the energy of soft photons setting $\omega = \sqrt{s}/2$.

The heavier fermions have less influence on the net result, and the top quark decouples nearly completely. Between 1 and 500 GeV the sum of boxes with factorizable diagrams with muon loops contributes, roughly speaking, at the order of permille to the net pure QED cross section, and the tau lepton contributes less. The Z resonance distorts this figure, by making the influence of two-loop contributions less influential for large-angle scattering where the resonance dominates.

\sqrt{s} [GeV]	1	10	M_Z	500
QED Born	440994	4409.94	53.0348	1.76398
rest e	193	5.73	0.1357	0.00673
μ	< 1	0.42	0.0408	0.00288
	\times	0.08	0.0407	0.00288
τ	< 1	< 10^{-2}	0.0027	0.00088
	\times	\times	-0.0096	0.00084
t	< 1	< 10^{-2}	< 10^{-4}	< 10^{-5}
	\times	\times	\times	\times

Table 1. Numerical values for the differential cross section in nanobarns at a scattering angle $\theta = 3^\circ$, in units of 10^2 ; $M_Z = 91.1876$ GeV. Bold-face entries are obtained with dispersion relations. The energy of the soft photon is chosen to be $\omega = \sqrt{s}/2$.

4. Summary

We have evaluated the $n_f = 2$ virtual two-loop corrections to Bhabha scattering due to fermions with arbitrary mass m_f in the limit of vanish-

\sqrt{s} [GeV]	1	10	M_Z	500
QED Born	466537	4665.37	56.1067	1.86615
full Born	466558	4686.27	1273.2680	0.85496
rest e	807	14.53	0.2706	0.01193
μ	160	6.08	0.1470	0.00726
	153	6.08	0.1470	0.00726
τ	2	1.33	0.0752	0.00457
	\times	1.07	0.0752	0.00457
t	< 1	$< 10^{-2}$	0.0005	0.00043
	\times	\times	\times	-0.00013

Table 2. Numerical values for the differential cross section in nanobarns at a scattering angle $\theta = 90^\circ$, in units of 10^{-4} . See Table 1 for further details.

ing electron mass m_e . We have not combined these (infrared finite) virtual contributions with those arising from irreducible vertices; the latter are logarithmically enhanced by terms of order up to $\ln^3(s/m_f^2)$, but are independent of $\ln(s/m_e^2)$, being collinear finite. They have to be assembled with the unresolved real heavy fermion emission, which is known to cancel the $\ln^3(s/m_f^2)$ and might lead to a suppression of the net effect. For the phenomenological analysis we will have also to take into account the effect of the running of the fine-structure constant. Concerning the results shown in the tables, the numerical contributions do not exceed the per mille level, and depend strongly on the kinematics. The formulae presented here apply to the leptons μ and τ , but also to the top quark. The latter decouples at small energies, but has to be taken into account at the ILC.

The determination of hadronic corrections is in preparation.

Note added:

After completion of this article, a draft [31] appeared, where the authors also study the fermionic corrections to Bhabha scattering with arbitrary masses of the internal fermions.

REFERENCES

- [1] T. Riemann, "Fermionic NNLO corrections to Bhabha scattering", talk held at this conference, <http://www.us.edu.pl/~us2007/talks.htm>
- [2] Z. Bern, L. Dixon, and A. Ghinculov, *Phys. Rev.* **D63** (2001) 053007, hep-ph/0010075.

- [3] N. Glover, B. Tausk, and J. van der Bij, *Phys. Lett.* **B516** (2001) 33–38, hep-ph/0106052.
- [4] A. Penin, *Phys. Rev. Lett.* **95** (2005) 010408, hep-ph/0501120.
- [5] A. Penin, *Nucl. Phys.* **B734** (2006) 185–202, hep-ph/0508127.
- [6] R. Bonciani, P. Mastrolia, and E. Remiddi, *Nucl. Phys.* **B661** (2003) 289–343, hep-ph/0301170.
- [7] R. Bonciani, P. Mastrolia, and E. Remiddi, *Nucl. Phys.* **B676** (2004) 399–452, hep-ph/0307295.
- [8] R. Bonciani, A. Ferroglia, P. Mastrolia, E. Remiddi, and J. van der Bij, *Nucl. Phys.* **B681** (2004) 261–291, hep-ph/0310333.
- [9] M. Czakon, J. Gluza, and T. Riemann, *Phys. Rev.* **D71** (2005) 073009, hep-ph/0412164.
- [10] R. Bonciani, A. Ferroglia, P. Mastrolia, E. Remiddi, and J. van der Bij, *Nucl. Phys.* **B701** (2004) 121–179, hep-ph/0405275.
- [11] R. Bonciani, A. Ferroglia, P. Mastrolia, E. Remiddi, and J. van der Bij, *Nucl. Phys.* **B716** (2005) 280–302, hep-ph/0411321.
- [12] S. Actis, M. Czakon, J. Gluza, and T. Riemann, *Nucl. Phys.* **B786** (2007) 26–51, arXiv:0704.2400v.2 [hep-ph].
- [13] T. Becher and K. Melnikov, *JHEP* **06** (2007) 084, arXiv:0704.3582 [hep-ph].
- [14] A. Mitov and S. Moch, *JHEP* **05** (2007) 001, hep-ph/0612149.
- [15] V. Smirnov, *Phys. Lett.* **B460** (1999) 397–404, hep-ph/9905323.
- [16] B. Tausk, *Phys. Lett.* **B469** (1999) 225–234, hep-ph/9909506.
- [17] M. Czakon, J. Gluza, and T. Riemann, *Nucl. Phys. (Proc. Suppl.)* **B135** (2004) 83, hep-ph/0406203.
- [18] G. Heinrich and V. Smirnov, *Phys. Lett.* **B598** (2004) 55–66, hep-ph/0406053.
- [19] M. Czakon, J. Gluza, and T. Riemann, *Nucl. Phys.* **B751** (2006) 1–17, hep-ph/0604101.
- [20] M. Czakon, A. Mitov, and S. Moch, *Phys. Lett.* **B651** (2007) 147–159, arXiv:0705.1975 [hep-ph].
- [21] G. Montagna, “Status of precision Monte Carlo tools for luminosity monitoring at meson factories”, talk held at this conference.
- [22] K. Kajda, “Pentagon diagrams of Bhabha scattering”, talk held at this conference and arXiv:0710.5100 [hep-ph].
- [23] J. Gluza, K. Kajda, and T. Riemann, *Comput. Phys. Commun.* **177** (2007) 879–893, arXiv:0704.2423 [hep-ph].
- [24] M. Czakon, *Comput. Phys. Commun.* **175** (2006) 559–571, hep-ph/0511200.
- [25] J. Vermaseren, “New features of FORM”, math-ph/0010025.
- [26] A. Arbuzov, D. Haidt, C. Matteuzzi, M. Paganoni, and L. Trentadue, *Eur. Phys. J.* **C34** (2004) 267–275, hep-ph/0402211.
- [27] B. Kniehl, M. Krawczyk, J. Kühn, R. Stuart, *Phys. Lett.* **B209** (1988) 337.
- [28] G. Burgers, *Phys. Lett.* **B164** (1985) 167.

- [29] D. Bardin *et al.*, *Comput. Phys. Commun.* **133** (2001) 229–395, hep-ph/9908433.
- [30] A. Arbuzov, M. Awramik, M. Czakon, A. Freitas, M. Grünewald, K. Mönig, S. Riemann, and T. Riemann, *Comput. Phys. Commun.* **174** (2006) 728–758, hep-ph/0507146.
- [31] R. Bonciani, A. Ferroglia and A. A. Penin, arXiv:0710.4775 [hep-ph]